

π -tons — generic optical excitations of correlated systems

A. Kauch^{a,*}, P. Pudleiner^{a,b,*}, K. Astleithner^a, T. Ribic^a, and K. Held^a

^a*Institute of Solid State Physics, TU Wien, 1040 Vienna, Austria and*

^b*Institute of Theoretical and Computational Physics, Graz University of Technology, 8010 Graz, Austria**

(Dated: July 17, 2022)

The interaction of light with solids gives rise to new bosonic quasiparticles, with the exciton being—undoubtedly—the most famous of these polaritons. While excitons are the generic polaritons of semiconductors, we show that for strongly correlated systems another polariton is prevalent—originating from the dominant antiferromagnetic or charge density wave fluctuations in these systems. As these are usually associated with a wave vector (π, π, \dots) or close to it, we propose to call the derived polaritons π -tons. These π -tons yield the leading vertex correction to the optical conductivity in all correlated models studied: the Hubbard, the extended Hubbard model, the Falicov-Kimball, and the Pariser-Parr-Pople model, both in the insulating and in the metallic phase.

Since the springtime of modern physics, the interaction of solids with light has been of prime interest. The arguably simplest kind of interaction is Einstein's Noble prize winning photoelectric effect [1], where the photon excites an electron across the band gap. More involved processes beyond a mere electron-hole excitation can be described in general by effective bosonic quasiparticles, coined polaritons since a polar excitation is needed to couple the solid to light.

The prime example of a polariton is the exciton [2, 3], where the excited electron-hole pair is bound due to the Coulomb attraction between electron and hole. This interaction is visualized in Fig. 1 (a). Since it is an attractive interaction, an exciton requires the exciton binding energy less than an unbound electron-hole pair. Other polaritons describe the coupling of the photon to surface plasmons, magnons or phonons.

Fig. 1 (b) describes the exciton in terms of Feynman diagrams: the incoming photon creates the electron-hole pair (distinguishable by the different [time] direction of the arrows) which interact with each other repeatedly and finally recombine emitting a photon. Since the energy-momentum relation of light is very steep compared to the electronic bandstructure of a solid, the transferred momentum from the photon is negligibly small $\mathbf{q} = 0$. Thus, electron and hole have the same momentum. For semiconductors this is often the preferable momentum transfer as well, connecting the bottom of the conduction with the top of the valence band as in Fig. 1 (a).

In this paper we show that the generic polaritons for strongly correlated systems are strikingly different. While semiconductors are band insulators with a filled valence and empty conduction band, strongly correlated systems are typically closer to a half-filled (or in general integer filled) band which is split into two Hubbard bands by strong electronic correlations as visualized in Fig. 1 (c) for a Mott insulator. (In case of a metallic system there is an additional quasiparticle band). Both metal and insulator are prone to strong antiferromagnetic (AFM)

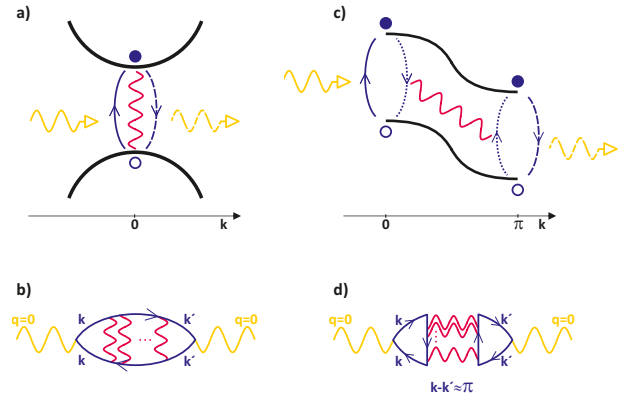


FIG. 1. (Color online) Sketch of the physical processes (top) and Feynman diagrams (bottom) behind an exciton (left) and a π -ton (right). The yellow wiggled line symbolizes the incoming (and outgoing) photon which creates an electron-hole pair denoted by open and filled circles, respectively. The Coulomb interaction between the particles is symbolized by a red wiggled line; dashed line indicates the recombination of the particle and hole; dotted line denotes the creation of a second particle-hole pair (right); black lines the underlying band-structure (top panels).

or charge density wave (CDW) fluctuations with a wave vector close to $\mathbf{q} = (\pi, \pi, \dots)$ [4, 5]. Indeed these fluctuations can be described by the central part of the Feynman diagram Fig. 1 (b), where the bare ladder diagrams correspond to the random phase approximation (RPA). However the wave vector $\mathbf{q} = (\pi, \pi, \dots)$ cannot directly couple to light, which only transfers $\mathbf{q} = 0$. Hence an exciton-like polariton as displayed in Fig. 1 (b) is not possible for AFM or CDW fluctuations.

As we will show in this paper, the (π, π, \dots) fluctuations nonetheless constitute the dominant vertex corrections beyond a bare (bubble) particle-hole excitation. This is possible through a process where the central part of the Feynman diagram Fig. 1 (b), i.e., the (π, π, \dots) fluctuations, are rotated (and flipped) as sketched in

Fig. 1 (d). Now it is possible to transfer $\mathbf{q} = 0$ from the photon and to pick up nonetheless the strong AFM or CDW fluctuations at $\mathbf{k} - \mathbf{k}' \approx (\pi, \pi, \dots)$. The physics of the associated process is visualized in Fig. 1 (c). First, the light creates an electron-hole pair. Because of the strong Coulomb interaction this electron-hole pair creates a second electron-hole pair at a wave vector displaced by (π, π, \dots) , and the two interact repeatedly with each other, before emitting a photon again. Note that if one assigns times to the electron-photon and Coulomb interactions in Fig. 1 (d) there are, after the first and till the last Coulomb interaction, always two particle and two hole Green's functions. This makes the π -ton distinctively different from excitons or quasiparticle-quasihole excitations, including those of a backfolded Brillouin zone envisaged as the coupling of AFM fluctuations to light in [6] where the importance of AFM fluctuations was realized.

This excitation resembles to some extent [7] the pairing of electrons in superconductors through magnetic fluctuations. Since AFM or CDW fluctuations are typically at or close to a wave vector (π, π, \dots) , we suggest to call this polariton a π -ton. But of course if a strongly correlated system happens to have its dominant fluctuations at another wave vector $\mathbf{k} - \mathbf{k}' \neq 0$, the same processes described in this paper allow for the coupling to light, creating polaritons.

In hindsight it appears rather obvious that AFM or CDW fluctuations couple this way to light. Why has this not been realized before? This is because numerical methods such as quantum Monte Carlo [6] or exact diagonalization [8] suffer from the difficulty to analyze the underlying physical processes, and analytical methods as e.g. RPA or FLEX [9] have been mostly biased with respect to certain channels such as the particle-hole (ph) channel in Fig. 1 (b) for excitons. Similar Feynman diagrams but with maximally crossed interaction lines, i.e., the particle-particle (pp) channel, have been made responsible for weak localization [10] and strong localization [11] in disordered systems. But the third (rotated) transversal particle-hole (\overline{ph}) channel of Fig. 1 (d) has, to the best of our knowledge, not been considered hitherto, except for the second order diagram, the Aslamazov-Larkin correction [12–14] which for half-filling compensates the second-order diagram of the pp -channel. Let us emphasize that it is however the whole ladder which is responsible for strong AFM or CDW fluctuations.

Our insight has only been possible because of recent methodological advances which allow us to study all three aforementioned channels unbiasedly, using the parquet equations [16–18] within the dynamical vertex approximation (DVA) [19–21], the dual fermion approach (DF) [22] and the parquet approximation (PA) [16]. For a review of these and related methods [23–26], see [27].

Models and methods. Let us now turn to the actual

calculations, starting with introducing the models, which all can be summarized in the Hamiltonian

$$\mathcal{H} = -t \sum_{\langle ij \rangle \sigma} c_{i\sigma}^\dagger c_{j\sigma} + U \sum_i n_{i\uparrow} n_{i\downarrow} + \frac{1}{2} \sum_{i \neq j, \sigma \sigma'} V_{ij} n_{i\sigma} n_{j\sigma'} \quad (1)$$

where $c_{i\sigma}^{(\dagger)}$ represents annihilation (creation) operator for an electron with spin σ at site i ; $n_{i\sigma} = c_{i\sigma}^\dagger c_{i\sigma}$; $\langle ij \rangle$ sums over each nearest neighbor pair i, j once. For the Hubbard model (HM) we have a local interaction U only, i.e., $V_{ij} = 0$, and t denotes the hopping. We also study the extended Hubbard model (ExtHM), with nearest-neighbor interaction $V_{ij} = V$. The Pariser-Parr-Pople model (PPP) [28, 29] describes conjugated π -bonds in carbon-based organic molecules and is here employed for a benzene ring, i.e., a one-dimensional chain with six sites, periodic boundary conditions and interactions between all sites. Finally, the Falicov-Kimball model (FKM) [30, 31] has the same form as the HM but the hopping is only for one spin species. All models are solved for the square lattice (except PPP) at half-filling in the paramagnetic phase; $t \equiv 1$ and Planck constant $\hbar \equiv 1$ set our unit of energies and frequencies; for the optical conductivity lattice constant $a \equiv 1$, elementary charge $e \equiv 1$.

We employ the method which we consider most appropriate for the four models, i.e., the parquet DVA for the HM [32], the PA for the ExtHM and PPP (which is here more precise than a non-self-consistent DVA [33, 34]), and a parquet variant of the DF, extending earlier DF approaches [35–37], [38]. We solve the parquet equations on a 6×6 momentum grid, except for the PPP for benzene which has 6 sites or momenta. For the HM, ExtHM and PPP we use the *victory* code [18] to solve the parquet equations, and *w2dynamics* [39] to calculate the fully irreducible vertex in case of the HM; for the FKM we employ a reduced frequency structure of the vertex [37] implemented in a special-purpose parquet code.

The optical conductivity $\sigma(\omega) = \Re \frac{\chi_{jj}^{\mathbf{q}=0}(\omega+i\delta) - \chi_{jj}^{\mathbf{q}=0}(i\delta)}{i(\omega+i\delta)}$, for $\delta \rightarrow 0$, is calculated from the current-current correlation function $\chi_{jj}^{\mathbf{q}=0}$ at Matsubara frequency ω_n and momentum $\mathbf{q} = 0$, which can be separated into a bubble term consisting of two Green's functions G_k only and vertex corrections $F_d^{kk'q}$ in the following way:

$$\chi_{jj,q} = \frac{2}{\beta N} \sum_k [\gamma_{\mathbf{k}}^{\mathbf{q}}]^2 G_{q+k} G_k + \frac{2}{(\beta N)^2} \sum_{k,k'} \gamma_{\mathbf{k}}^{\mathbf{q}} \gamma_{\mathbf{k}'}^{\mathbf{q}} G_{k'} G_{q+k} F_d^{kk'q} G_{q+k'} G_k \quad (2)$$

Here and in the following, we use a four-vector notation $k = (\mathbf{k}, \nu_n)$ with $q = (\mathbf{q} = 0, \omega_n)$; $\gamma_{\mathbf{k}}^{\mathbf{q}=0} = \partial \epsilon_{\mathbf{k}} / \partial \mathbf{k}$ denotes the dipole matrix elements given by the derivative of the energy-momentum relation in the Peierls approximation [40].

In the parquet-based approaches employed, the vertex F contains contributions from the fully irreducible ver-

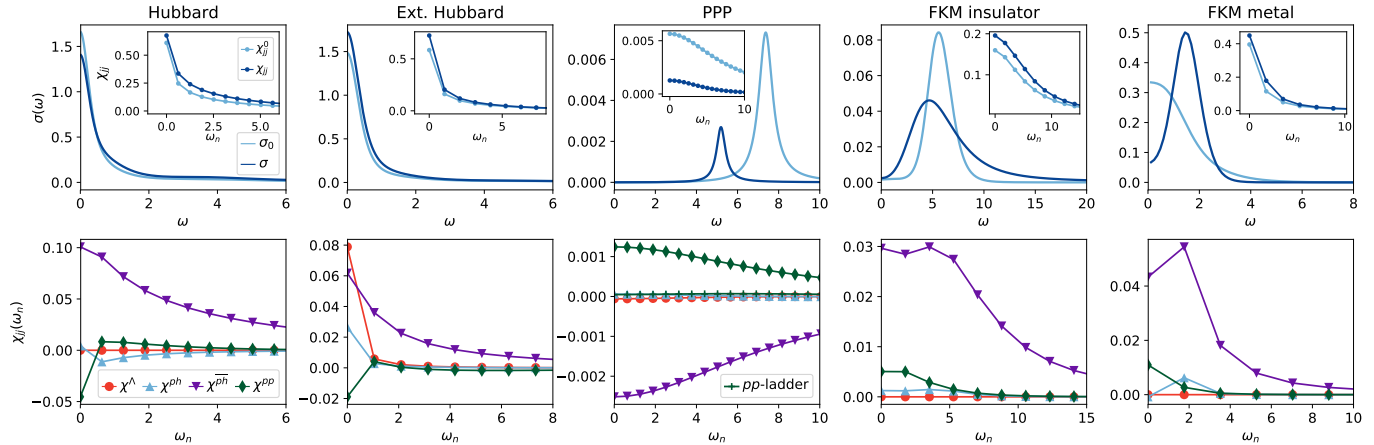


FIG. 2. (Color online) Top: Optical conductivity for real frequency (main panel) and the corresponding current-current correlation function in Matsubara frequencies (insets) of the five cases studied, showing the bare bubble (σ_0) and the full conductivity (σ) including vertex corrections (in the insets χ_{jj}^0 and $\overline{\chi}_{jj}$, respectively). Bottom: Corresponding vertex correction to the current-current correlation function χ_{jj} separated into ph , \overline{ph} , pp and Λ contributions. For the PPP also the contribution of a RPA-like pp -ladder is shown. Parameters from left to right: $U = 4t$, $T = 0.1t$ (HM); $U = 4t$, $T = 0.17t$, $V = t$ (ExtHM); $T = 0.1t$, $U = 3.962t$, $V_{01} = 2.832t$, $V_{02} = 2.014t$, $V_{03} = 1.803t$ (PPP; interactions translated into units of t are fitted to experiment [15]); $U = 6t$, $T = 0.28t$ (FKM insulator); $U = 2t$, $T = 0.28t$ (FKM metal).

tex Λ as well as contributions that are reducible in the three channels (ph , \overline{ph} , pp): $F = \Lambda + \Phi_{ph} + \Phi_{\overline{ph}} + \Phi_{pp}$ [41]. The density component F_d that enters the optical conductivity denotes the even spin combination [17, 27].

Inserting in Eq. 2 instead of F one of the summands Λ , $\Phi_{ph/\overline{ph}/pp}$ we obtain the contributions from the respective channels: χ^Λ , χ^{ph} , $\chi^{\overline{ph}}$, and χ^{pp} . The most simple contributions to χ^{ph} and $\chi^{\overline{ph}}$ are just the ladder diagrams of Fig. 1 (b) and (d), respectively. For the analytic continuation of the optical conductivity to real frequencies we employ the maximum entropy method [42]; for the PPP we used Padé interpolation.

Results: Optical Conductivity. Let us now turn to the results, starting with the optical conductivity in Fig. 2 (top). Within the four models, we studied five physically different examples: HM (metal), ExtHM (metal), PPP (insulator), FKM (insulator), and FKM (metal) [see Supplemental Material (SM) for results at different parameters]. In all five cases we see noticeable vertex corrections. For the two insulators, especially for the PPP, there is a strong reduction of the optical gap compared to the one-particle gap (bare bubble contribution σ_0). Usually one would associate such a reduction to the exciton binding energy. However, when inspecting the contribution of the individual channels in Fig. 2 (bottom), we see that it is not the ph -channel of the exciton but the \overline{ph} -channel which is dominating and responsible for the reduction of the optical gap. Note that a ph -ladder built from a local interaction (RPA) or a local vertex (as e.g. in dynamical mean field theory [43]) has zero contribution to the optical conductivity [44]. This is why we included in our study also the PPP and ExtHM where through non-local

interaction one obtains simple ladder contributions in the ph -channel [45].

For two of the metallic cases (HM and FKM) the vertex corrections reduce the conductivity at small frequencies. One might be tempted to associate this with weak localization corrections, i.e., the pp -channel. But again by inspecting the vertex contributions in Fig. 2 (bottom) we see that it is the \overline{ph} -channel that is dominating; the pp contribution is small. The third metallic case (ExtHM) is different in the sense that, besides the \overline{ph} -channel, the bare vertex Λ contributes to a similar amount. This is because the non-local interaction provides an additional way to polarize the system and hence to couple to light.

In all cases except for the ExtHM, the pp -channel provides the second largest contribution. One might suspect that this stems from simple RPA-like ladder diagrams as envisaged in the theory of weak localization. But this is not the case. In the case where this pp -channel is largest, i.e., for the PPP, we additionally plot the contribution from a bare RPA-like pp -ladder. It is negligibly small.

Physical origin of vertex corrections. Why does the \overline{ph} -channel give such a big contribution? It is because of the dominant fluctuations in the system. These are AFM or CDW fluctuations at a wave vector (π, π, \dots) (see below). These fluctuations are already generated by RPA-ladder diagrams in the ph -channel and in the \overline{ph} -channel as visualized in Fig. 1. Let us emphasize however, that the employed parquet methods take many more Feynman diagrams and the mutual coupling of these channels into account.

The fact that the bare pp -ladder in Fig. 2 (bottom middle) is small shows us that there is a strong feedback of the AFM or CDW fluctuations into the pp -channel

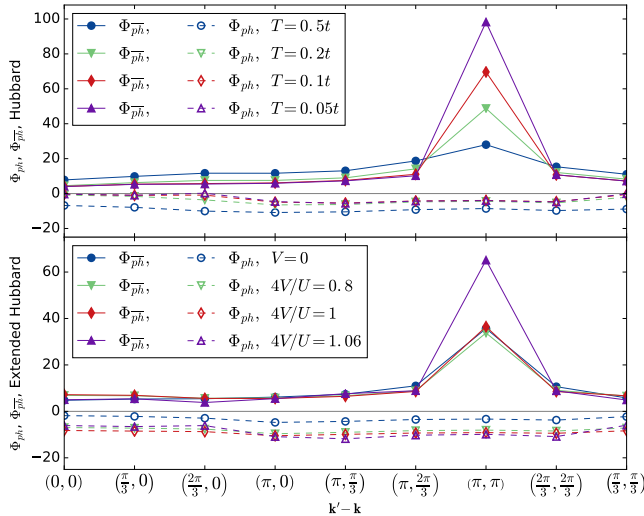


FIG. 3. (Color online) Reducible contributions Φ in the ph and $\bar{p}h$ -channel to the full vertex $F_{d,\mathbf{k}\mathbf{k}'\mathbf{q}=0}^{\nu_n\nu'_n\omega_n}$ correcting the optical conductivity. Top: HM at various temperatures and $U = 4t$. Bottom: ExtHM at $U = 4t$, $T = 0.17t$ and various V . Shown is the contribution $\nu_n = \nu'_n = \pi T$; $\omega_n = 0$ at fixed $\mathbf{k} = 0$ as a function of $\mathbf{k}' - \mathbf{k}$.

through the parquet equations, which leads to the considerable contributions of the pp -channel. In other words, these pp contributions arise (only) as a consequence of the enhanced AFM and CDW fluctuations.[46]

To demonstrate the importance of the (π, π) contribution, we plot in Fig. 3 the reducible contributions Φ to the full vertex F as a function of $\mathbf{k}' - \mathbf{k}$ for the ph and $\bar{p}h$ -channel, setting $\mathbf{q} = 0$ for the optical conductivity. Note that the reducible ph and $\bar{p}h$ vertices are interrelated, i.e., $\Phi_{\bar{p}h,d,\mathbf{k}\mathbf{k}'\mathbf{q}=0}^{\nu_n\nu'_n\omega_n} = -\frac{1}{2}(\Phi_{ph,d} + 3\Phi_{ph,m})_{\mathbf{k}\mathbf{k}'-\mathbf{k}}^{\nu_n\nu_n+\omega_n\nu'_n-\nu_n}$ with d (m) denoting the even (odd) spin combination [17, 27], but the part of the ph -channel that enters the optical conductivity is a very different one: $\Phi_{ph,(ph),d,\mathbf{k}\mathbf{k}'\mathbf{q}=0}^{\nu_n\nu'_n\omega_n}$. As we see in Fig. 3 this ph -contribution is small and the $\bar{p}h$ -contribution is strongly peaked at the wave vector $\mathbf{k}' - \mathbf{k} = (\pi, \pi)$ because of the strong AFM and CDW fluctuations for the HM and ExtHM, respectively. Hence we can conclude that it is indeed predominately the $\mathbf{k}' - \mathbf{k} = (\pi, \pi)$ contribution that is responsible for the vertex corrections in the optical conductivity, and therefore we call these polaritons π -tons.

A similar peak at $\mathbf{k}' - \mathbf{k}$ in the $\bar{p}h$ -channel is also found for the PPP in Fig. 4, where we only have six momenta so that we can additionally show the dependence on the Matsubara frequencies. This confirms the picture of the π -tons feeding upon strong AFM or CDW fluctuations.

Interesting questions which can however not finally be answered at the moment are: Has the π -ton a peak at a single frequency ω like an exciton or does the light rather couple to a continuum of bosonic excitations with different ω 's for different \mathbf{k} 's in Eq. (2)? In the latter case,

do the π -tons rather shift the quasiparticle-quasihole excitation spectrum or result in additional peaks for every \mathbf{k} ?

Characteristics of the π -ton. While AFM and CDW fluctuations are dominant at all parameters and temperatures analyzed, they become—as a matter of course—stronger when we approach a corresponding phase transition. This effect can be seen in Fig. 3 For the HM (top panel of Fig. 3), reducing the temperature means that AFM fluctuations become strongly enhanced, cf. [21, 35, 47–49]. While there is no finite-temperature phase transition in two dimensions, the correlation length becomes exponentially large [50]. For the ExtHM, Fig. 3 (bottom), we instead enhance the non-local interaction V . This way we approach a phase transition towards CDW ordering (at $4V = U$ in the atomic limit and at a slightly larger V 's here [34]).

Conclusion and outlook. We have provided compelling evidence for what appears to be the generic polaritons in strongly correlated electron systems—at least in one and two dimensions. These polaritons, coined π -tons, consist of two particle-hole pairs coupled to the incoming and outgoing light, respectively, and glued together by AFM and CDW fluctuations.

Although the optical conductivity has been studied for a wide range of materials [51–56], it is difficult to quantify vertex corrections and even more difficult to rule out that these stem from excitons or weak localization corrections. If we enhance AFM or CDW fluctuations by reducing temperature or by approaching a phase transition the one-particle physics and the one-particle gap will be modified as well because of the onset of AFM or CDW order including additional spin polaron peaks [57, 58], by enhanced life times in a Fermi liquid or by emergent pseudogap physics [59]. Against this background, we feel that a combination of optical experiments with angular resolved photoemission spectroscopy (ARPES) or neutron scattering and accompanying theoretical calculations is needed to identify π -tons in experiment. A characteristic of at least AFM π -tons will also be a high sensitivity of the optical gap to an external magnetic field.

Acknowledgements. We would like to thank Jan Kunes, Gang Li, Patrik Thunström, and Angelo Valli for many stimulating discussions, Josef Kaufmann for the help with analytical continuation, and Monika Waas for graphical assistance. The present work was supported by the European Research Council under the European Union's Seventh Framework Program (FP/2007-2013) through ERC Grant No. 306447, the Austrian Science Fund (FWF) through project P 30997-N32 and Doctoral School “Building Solids for Function” (P.P.). Calculations have been done on the Vienna Scientific Cluster (VSC).

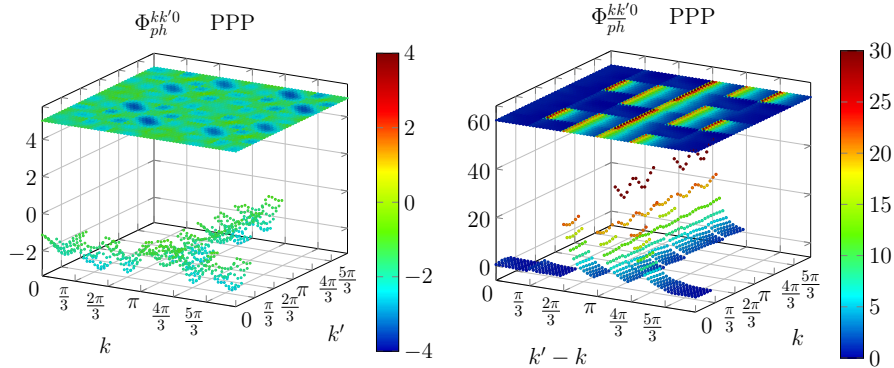


FIG. 4. (Color online) Reducible contributions Φ in the ph (left) and $\bar{p}h$ -channel (right) entering the optical conductivity as vertex corrections plotted vs. the four-vectors k and k' or $k' - k$, respectively. For each combination of momenta, the dependence on frequencies is plotted on the finer scale (bosonic frequency $\omega_n = 0$). Parameters as in Fig. 2.

* These authors contributed equally to this work

- [1] A. Einstein, *Annalen der Physik* **322**, 132 (1905).
- [2] J. Frenkel, *Phys. Rev.* **37**, 17 (1931).
- [3] G. H. Wannier, *Phys. Rev.* **52**, 191 (1937).
- [4] B. Keimer, “Autumn School on Correlated Electrons.emergent phenomena in correlated matter,” (Forschungszentrum Jülich, 2013) Chap. Recent Advances in Experimental Research on High-Temperature Superconductivity.
- [5] G. Aeppli, *Journal of Magnetism and Magnetic Materials* **272-276**, 7 (2004).
- [6] N. Lin, E. Gull, and A. J. Millis, *Phys. Rev. B* **80**, 161105 (2009).
- [7] There are however differences. In a superconductor there are two particles involved that interact through repeated ladders. Here we have two electron-hole pairs that interact through one ladder.
- [8] J. Vucicevic, J. Kokalj, R. Zitko, N. Wentzell, D. Tanaskovic, and J. Mravlje, arXiv e-prints , arXiv:1811.08343 (2018), arXiv:1811.08343 [cond-mat.str-el].
- [9] H. Kontani, *Journal of the Physical Society of Japan* **75**, 013703 (2006), <https://doi.org/10.1143/JPSJ.75.013703>.
- [10] B. L. Altshuler and A. G. Aronov, *Electron-Electron interaction in disordered conductors*, edited by A. I. Efros and M. Pollak (Elsevier Science Publisher, 1985).
- [11] E. Abrahams, P. W. Anderson, D. C. Licciardello, and T. V. Ramakrishnan, *Phys. Rev. Lett.* **42**, 673 (1979).
- [12] L. G. Aslamazov and A. I. Larkin, *Sov. Phys. Solid State* **10**, 875 (1968).
- [13] D. Bergeron, V. Hankevych, B. Kyung, and A.-M. S. Tremblay, *Phys. Rev. B* **84**, 085128 (2011).
- [14] A. V. Chubukov, D. L. Maslov, and V. I. Yudson, *Phys. Rev. B* **89**, 155126 (2014).
- [15] R. J. Bursill, C. Castleton, and W. Barford, *Chem. Phys. Lett.* **294**, 305 (1998).
- [16] N. E. Bickers, “Theoretical methods for strongly correlated electrons,” (Springer-Verlag New York Berlin Heidelberg, 2004) Chap. 6, pp. 237–296.
- [17] G. Li, N. Wentzell, P. Pudleiner, P. Thunström, and K. Held, *Phys. Rev. B* **93**, 165103 (2016).
- [18] G. Li, A. Kauch, P. Pudleiner, and K. Held, arXiv:1708.07457 (2017), arXiv:1708.07457.
- [19] A. Toschi, A. A. Katanin, and K. Held, *Phys Rev. B* **75**, 045118 (2007).
- [20] H. Kusunose, *J. Phys. Soc. Jpn.* **75**, 054713 (2006).
- [21] A. A. Katanin, A. Toschi, and K. Held, *Phys. Rev. B* **80**, 075104 (2009).
- [22] A. N. Rubtsov, M. I. Katsnelson, and A. I. Lichtenstein, *Phys. Rev. B* **77**, 033101 (2008).
- [23] G. Rohringer, A. Toschi, H. Hafermann, K. Held, V. I. Anisimov, and A. A. Katanin, *Phys. Rev. B* **88**, 115112 (2013).
- [24] C. Taranto, S. Andergassen, J. Bauer, K. Held, A. Katanin, W. Metzner, G. Rohringer, and A. Toschi, *Phys. Rev. Lett.* **112**, 196402 (2014).
- [25] T. Ayril and O. Parcollet, *Phys Rev. B* **92**, 115109 (2015).
- [26] G. Li, *Phys. Rev. B* **91**, 165134 (2015).
- [27] G. Rohringer, H. Hafermann, A. Toschi, A. A. Katanin, A. E. Antipov, M. I. Katsnelson, A. I. Lichtenstein, A. N. Rubtsov, and K. Held, *Rev. Mod. Phys.* **90**, 025003 (2018).
- [28] J. A. Pople, *Trans. Faraday Soc.* **49**, 1375 (1953).
- [29] R. Pariser and R. G. Parr, *Journal of Chemical Physics* **21**, 466 (1953).
- [30] L. M. Falicov and J. C. Kimball, *Phys. Rev. Lett.* **22**, 997 (1969).
- [31] J. K. Freericks and V. Zlatić, *Rev. Mod. Phys.* **75**, 1333 (2003).
- [32] A. Kauch, F. Hörbinger, G. Li, and K. Held, arXiv e-prints , arXiv:1901.09743 (2019), arXiv:1901.09743 [cond-mat.str-el].
- [33] P. Pudleiner, P. Thunström, A. Valli, A. Kauch, G. Li, and K. Held, arXiv e-prints , arXiv:1812.04962 (2018), arXiv:1812.04962 [cond-mat.str-el].
- [34] P. Pudleiner, A. Kauch, K. Held, and G. Li, (2019), in preparation.
- [35] J. Otsuki, H. Hafermann, and A. I. Lichtenstein, *Phys. Rev. B* **90**, 235132 (2014).
- [36] S.-X. Yang, P. Haase, H. Terletska, Z. Y. Meng, T. Pruschke, J. Moreno, and M. Jarrell, *Phys. Rev. B* **89**, 195116 (2014).
- [37] T. Ribic, G. Rohringer, and K. Held, *Phys. Rev. B* **93**, 195105 (2016).
- [38] Note that the FKM is difficult to solve in DGA as the latter requires a mixed vertex with mobile and immobile electrons [37, 60].
- [39] M. Wallerberger, A. Hausoel, P. Gunacker, A. Kowalski, N. Parragh, F. Goth, K. Held, and G. Sangiovanni, *Computer Physics Communications* **235**, 388 (2019).
- [40] With the exception of the PPP for which we show the results for $\gamma_{\mathbf{k}} \equiv 1$, which corresponds to the dynamical compressibility. Additional results for $\gamma_{\mathbf{k}}^{a=0} = \partial \epsilon_{\mathbf{k}} / \partial \mathbf{k}$ are shown in SM.

- [41] A similar analysis of the contributions from different channels but for the self-energy has been done in [61].
- [42] D. Geffroy, J. Kaufmann, A. Hariki, P. Gu-nacker, A. Hausoel, and J. Kunes, arXiv e-prints , arXiv:1808.08046 (2018), arXiv:1808.08046 [cond-mat.str-el].
- [43] A. Georges, G. Kotliar, W. Krauth, and M. J. Rozen-berg, *Rev. Mod. Phys.* **68**, 13 (1996).
- [44] Because $G_{q+k}G_k$ in Eq. (2) is even in \mathbf{k} for $\mathbf{q} = 0$ and $\gamma_{\mathbf{k}}^{q=0}$ is odd.
- [45] Note that the non-zero ph contributions in the HM and FKM stem from insertions of other diagrams into the ph -ladder through the parquet equations.
- [46] In contrast, the bare ph -ladder would be much larger without feedback from the other channels.
- [47] G. Rohringer, A. Toschi, A. Katanin, and K. Held, *Phys. Rev. Lett.* **107**, 256402 (2011).
- [48] T. Schäfer, A. A. Katanin, K. Held, and A. Toschi, *Phys. Rev. Lett.* **119**, 046402 (2017).
- [49] J. Gukelberger, E. Kozik, and H. Hafermann, *Phys. Rev. B* **96**, 035152 (2017).
- [50] T. Schäfer, F. Geles, D. Rost, G. Rohringer, E. Arrigoni, K. Held, N. Blümer, M. Aichhorn, and A. Toschi, *Phys. Rev. B* **91**, 125109 (2015).
- [51] D. N. Basov, R. D. Averitt, D. van der Marel, M. Dressel, and K. Haule, *Rev. Mod. Phys.* **83**, 471 (2011).
- [52] S. Uchida, T. Ido, H. Takagi, T. Arima, Y. Tokura, and S. Tajima, *Phys. Rev. B* **43**, 7942 (1991).
- [53] S. Tajima, *Reports on Progress in Physics* **79**, 094001 (2016).
- [54] P. Lunkenheimer, F. Mayr, and A. Loidl, *Annalen der Physik* **15**, 498 (2006).
- [55] I. Lo Vecchio, L. Baldassarre, F. D’Apuzzo, O. Limaj, D. Nicoletti, A. Perucchi, L. Fan, P. Metcalf, M. Marsi, and S. Lupi, *Phys. Rev. B* **91**, 155133 (2015).
- [56] J. Ruppen, J. Teyssier, I. Ardizzone, O. E. Peil, S. Catalano, M. Gibert, J.-M. Triscone, A. Georges, and D. van der Marel, *Phys. Rev. B* **96**, 045120 (2017).
- [57] G. Sangiovanni, A. Toschi, E. Koch, K. Held, M. Capone, C. Castellani, O. Gunnarsson, S.-K. Mo, J. W. Allen, H.-D. Kim, A. Sekiyama, A. Yamasaki, S. Suga, and P. Metcalf, *Phys. Rev. B* **73**, 205121 (2006).
- [58] C. Taranto, G. Sangiovanni, K. Held, M. Capone, A. Georges, and A. Toschi, *Phys. Rev. B* **85**, 085124 (2012).
- [59] T. Timusk and B. Statt, *Rep. Prog. Phys.* **62**, 61 (1999).
- [60] T. Ribic, G. Rohringer, and K. Held, *Phys. Rev. B* **95**, 155130 (2017).
- [61] O. Gunnarsson, T. Schäfer, J. P. F. LeBlanc, E. Gull, J. Merino, G. Sangiovanni, G. Rohringer, and A. Toschi, *Phys. Rev. Lett.* **114**, 236402 (2015).

Supplemental material: π -tons — generic optical excitations of correlated systems

A. Kauch^{a,*}, P. Pudleiner^{a,b,*}, K. Astleithner^a, T. Ribic^a, and K. Held^a

^a*Institute of Solid State Physics, TU Wien, 1040 Vienna, Austria*

^b*Institute of Theoretical and Computational Physics, Graz University of Technology, 8010 Graz, Austria*

(Dated: July 17, 2022)

In this Supplemental Material, we present additional results for the optical conductivity and the corresponding current-current correlation function separated into different channels as the parameters of the models are varied. We also show the reducible contributions Φ_{ph}^- and Φ_{ph} to the full vertex F_d for the Falicov-Kimball model.

In the HM (Fig. S1) and FKM (Figs. S3-S4) we approach the AFM or CDW transition by lowering the temperature (in case of HM the AFM transition is at $T = 0$; in case of FKM the CDW transition is around $T = 0.12t$ for the metal with $U = 2t$ and around $T = 0.2t$ for the insulator with $U = 6t$ [37]), whereas for the ExtHM (Fig. S2) we approach the CDW transition by increasing the nearest-neighbor interaction V (the transition to CDW is around $V = 1.06t$ [34]). In all cases studied, as we approach the phase transition the vertex contribution becomes larger. As shown in the bottom panels of Figs. S1-S4 the largest overall contribution to the vertex part is $\chi^{\overline{ph}}$ (except PPP in Fig. S2, where it is χ^{pp}), with the second biggest being χ^{pp} (with the exception of the ExtHM in Fig. S2, where it is χ^Λ). However, as explained in the main text, the large values of χ^{pp} mainly come from insertions of other diagrams into the pure RPA-like pp -ladder that are generated in the parquet solution (for comparison see the bottom middle left plot in Fig. S1 and the bottom right of Fig. S2, where the contribution from a pp -ladder without other diagrammatic insertions is shown).

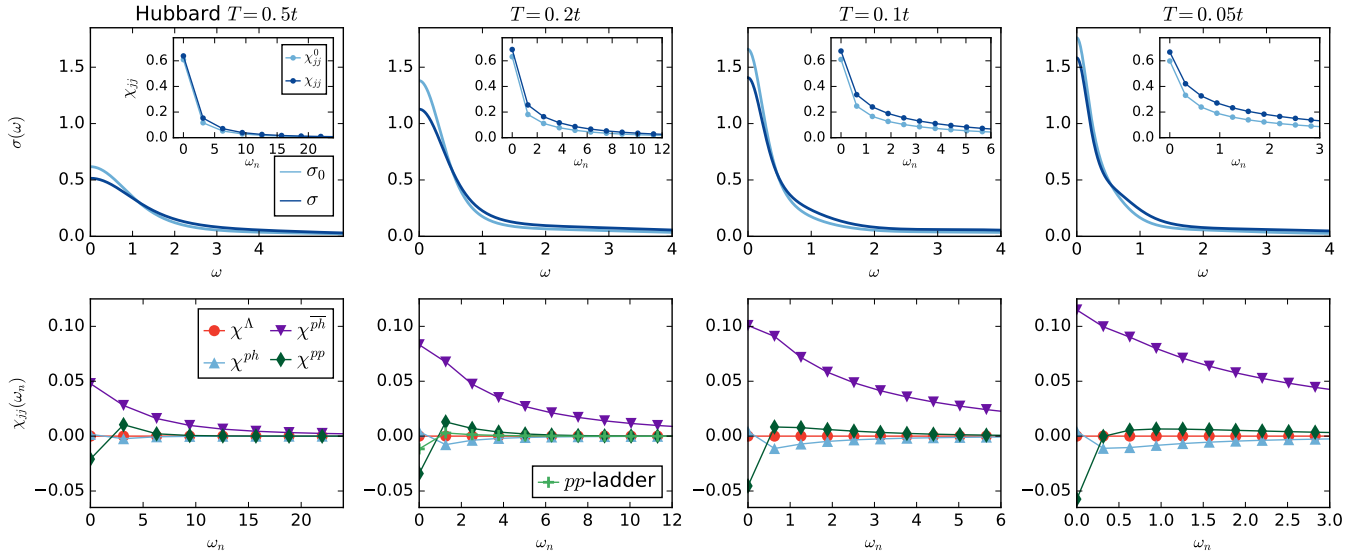


FIG. S1. Top: Optical conductivity for real frequency (main panel) and the corresponding current-current correlation function in Matsubara frequencies (insets) of the Hubbard model, showing the bare bubble (σ_0) and the full conductivity (σ) including vertex corrections (in the insets χ_{jj}^0 and χ_{jj} , respectively). Bottom: Corresponding vertex correction to the current-current correlation function χ_{jj} separated into the contributions from the three channels (ph , \overline{ph} , pp) as well as the fully irreducible contribution (Λ). From left to right different temperatures are shown at $U = 4t$. For $T = 0.2t$ also the contribution of a RPA-like pp ladder is shown. Other parameters as in the main paper.

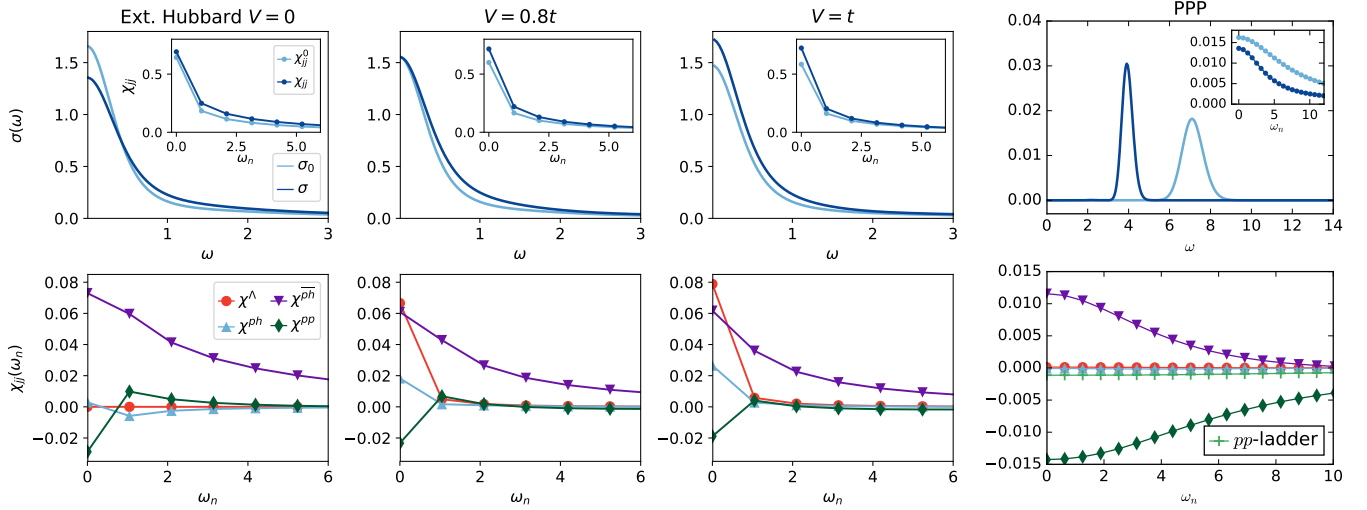


FIG. S2. The same as Fig. S1 but for the ExtHM and PPP model. From left to right different nearest neighbor interactions V are shown. The rightmost column is for the PPP with the electric field along the ring (i.e. $\gamma_{\mathbf{k}}^{\mathbf{q}=0} = \partial \epsilon_{\mathbf{k}} / \partial \mathbf{k}$). For the PPP also the contribution of a RPA-like pp ladder is shown. Other parameters are the same as in the main paper.

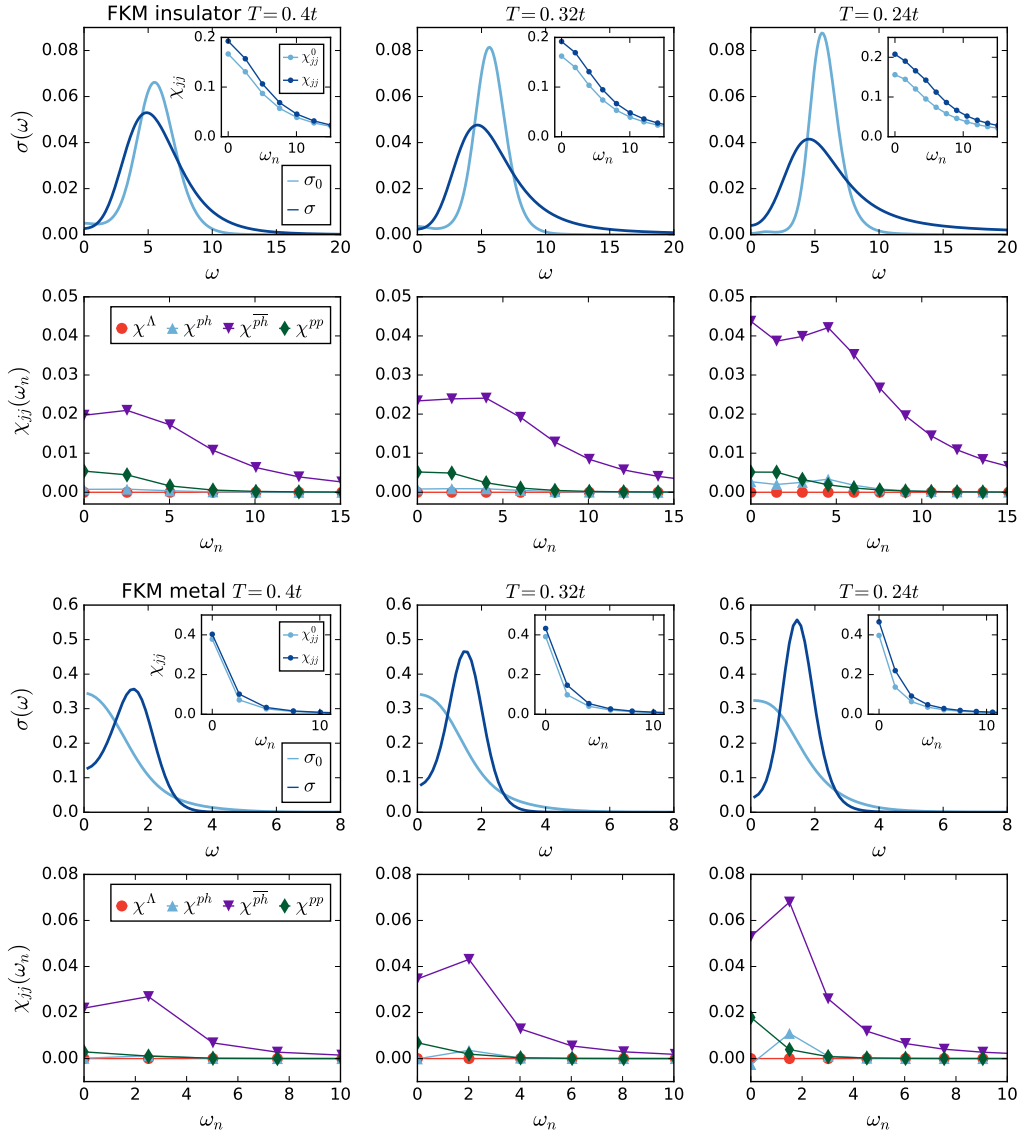


FIG. S3. The same as Fig. S1 but for the FKM at $U = 6t$ (insulator). From left to right different temperatures are shown. Other parameters are the same as in the main paper.

FIG. S4. The same as Fig. S1 but for the FKM at $U = 2t$ (metal). From left to right different temperatures are shown. Other parameters are the same as in the main paper.

We also show in Figs. S5-S6 the reducible contributions $\Phi_{\overline{ph}}$ and Φ_{ph} to the full vertex F_d for the FKM in the metallic (Fig. S5) and insulating (Fig. S6) phase. Also in this case, similarly as for the HM, ExtHM and PPP model shown in the main text, the $\mathbf{k}' - \mathbf{k} = (\pi, \pi)$ contribution to $\Phi_{\overline{ph}}$ is the largest. As we approach the phase transition, it grows, whereas the Φ_{ph} stays small and does not depend on $\mathbf{k}' - \mathbf{k} = (\pi, \pi)$ much, except for the lowest temperature of $T = 0.2t$ in Fig. S5 where a small $\mathbf{k}' - \mathbf{k}$ dependence develops.

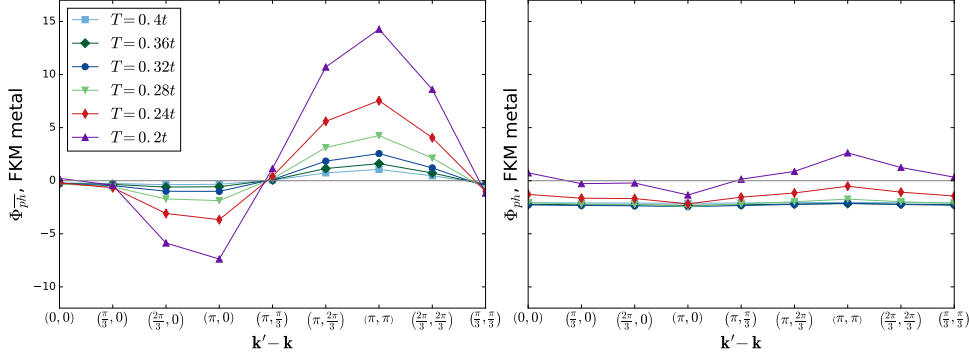


FIG. S5. Reducible contributions Φ in the \overline{ph} (left) and ph (right) channel to the full vertex $F_{d, \mathbf{k}\mathbf{k}'\mathbf{q}=0}^{\nu_n \nu'_n \omega_n}$ correcting the optical conductivity for the FKM at various temperatures and $U = 2t$ (metal). Shown is the contribution $\nu_n = \nu'_n = \pi T$; $\omega_n = 0$ at fixed $\mathbf{k} = (0, 0)$ as a function of $\mathbf{k}' - \mathbf{k}$.

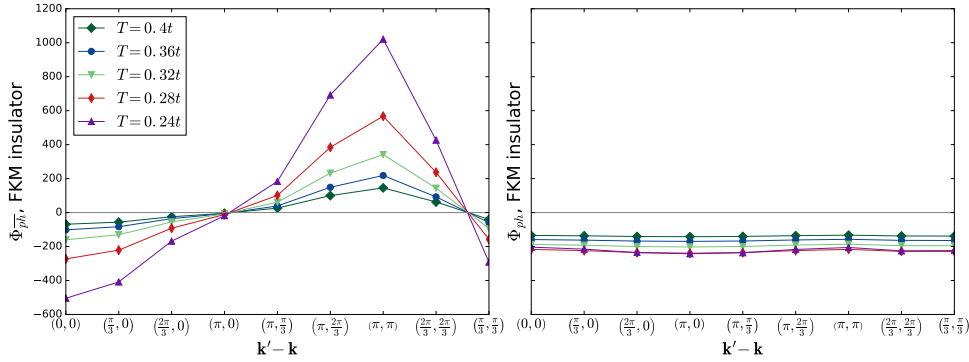


FIG. S6. The same as Fig. S5 but for $U = 6t$ (insulator).